

Role of zero-point effects in stabilizing the ground state structure of bulk Fe₂P

Soumya S. Bhat, Kapil Gupta, Satadeep Bhattacharjee and Seung Cheol Lee*

Indo-Korea Science and Technology Center (IKST), Bangalore 560065, India

(Dated: July 6, 2018)

Structural stability of Fe₂P is investigated in detail using first-principles calculations based on density functional theory. While the orthorhombic C23 phase is found to be energetically more stable, the experiments suggest it to be hexagonal C22 phase. In the present study, we show that in order to obtain the correct ground state structure of Fe₂P from the first-principles based methods it is utmost necessary to consider the zero-point effects such as zero-point vibrations and spin fluctuations. This study demonstrates an exceptional case where a bulk material is stabilized by quantum effects, which are usually important in low-dimensional materials. Our results also indicate the possibility of magnetic field induced structural quantum phase transition in Fe₂P, which should form the basis for further theoretical and experimental efforts.

I. INTRODUCTION

Fe₂P has attracted tremendous technological importance as it shows unique magnetic properties such as large uniaxial magnetocrystalline anisotropy [1], magnetocaloric [2, 3] and magnetoelastic [4] properties, due to which it finds wide use in industrial applications. In recent years, it has been also identified as potential electrocatalyst for hydrogen evolution reaction [5, 6]. Besides industrial significance, Fe₂P is also interesting to geophysicists as a major component of meteorites in the form of barringerite and allabogdanite minerals [7].

In view of its importance, many theoretical and experimental efforts are devoted to study the magnetic and catalytic properties of Fe₂P [2, 3, 8, 9], yet its elemental property such as thermodynamic structural stability is hardly discussed in literature. At ambient conditions, Fe₂P crystallizes in hexagonal C22-type structure with space group $P\bar{6}2m$ [10]. An early high pressure and high temperature X-ray diffraction experiment on Fe₂P by Senateur *et al.* [11], disclosed the presence of orthorhombic C23-type polymorph of Fe₂P with space group $Pnma$, under compression. This was later confirmed by recent experiments [12, 13], where Fe₂P is reported to undergo structural phase transition from C22 to C23 structure under pressure of 8 GPa upon heating to 1400 K. On the contrary, first-principles calculations based on density functional theory (DFT) predicted C23 structure as the stable phase of Fe₂P [14]. The discrepancy in the experimental observation and theoretical prediction of ground state structure of Fe₂P makes it essential to carry out a systematic analysis.

As stated earlier, in contrast to the experimental observation, theory predicts C23 structure as ground state of Fe₂P and there are no systematic studies on the structural stability of Fe₂P reported in literature. To fill this gap between the theory and experiment, we investigate the structural stability of Fe₂P using first-principles calculations based on DFT. Through comparison of struc-

tural parameters and magnetic properties of C22 and C23 phases, we analyze their consequences to stability. By determining full phonon spectra of C22 and C23 structures, we provide insights into the vibrational free energy contribution to the stability of C22 phase. Further, we determine ferromagnetic susceptibilities and compare zero-point spin fluctuation energies for both phases with implication to its ground state stability.

II. COMPUTATIONAL DETAILS

We performed first-principles calculations using the projector-augmented wave (PAW) [15] method in the framework of DFT as implemented in VASP code [16, 17]. The exchange-correlation energy of electrons is treated within a generalized gradient approximated functional (GGA) of the Perdew-Burke-Ernzerhof (PBE) [18] parametrized form. Interactions between ionic cores and valence electrons are represented using PAW pseudopotentials, where 4s, 3d electrons for Fe and 3s, 3p electrons for P are treated as valence. Plane-wave basis set with kinetic energy cutoff of 600 eV and an energy convergence criteria of 10⁻⁶ eV are used. Uniform meshes of 9x9x15 and 8x16x8 k-points are used for Brillouin zone sampling of hexagonal and orthorhombic unit cells, respectively. Phonon frequencies across the Brillouin zone are obtained using finite-displacement approach as implemented in the Phonopy code [19]. We used 2x2x3 and 2x3x2 supercells for C22 and C23 structures, respectively. The forces induced by small displacements are calculated using VASP, with 10⁻⁸ eV as energy convergence criterion.

III. RESULTS AND DISCUSSION

A. Electronic structure

For our calculations, initial structures are taken from experimental data [10, 11] and are optimized by full relaxation of the unit cell and atomic positions. The unit

* seungcheol.lee@ikst.res.in

TABLE I: Calculated unit cell parameters, magnetic stabilization energies and magnetic moments for C22 and C23 structures of Fe₂P, along with experimental data from literature

	C22		C23	
	This work	Expt. ^a	This work	Expt. ^b
a (Å)	5.81	5.87	5.61	5.78
b (Å)	–	–	3.57	3.57
c (Å)	3.43	3.46	6.51	6.64
V (Å ³)	100.2	103.1	130.4	136.9
$\Delta E^{\text{NM-FM}}$ (eV/f.u.)	0.22	–	0.18	–
μ^{Fe1} (μ_{B} /atom)	0.82	0.96	0.18	–
μ^{Fe2} (μ_{B} /atom)	2.23	2.31	1.61	–
$\mu^{\text{f.u.}}$ (μ_{B} /f.u.)	3.01	3.27	1.75	–

^a Refs. [10, 20].

^b Ref. [11].

cell of hexagonal C22 phase composed of three formula units, with six Fe and three P atoms. The Fe atoms occupy two non-equivalent threefold symmetry sites Fe(I) and Fe(II), while the P atoms are situated on one twofold, P(I) and on one single-fold P(II) position in the crystal lattice. Fe(I) atom is surrounded by four P atoms with tetrahedral symmetry, whereas Fe(II) atom is surrounded by five P atoms, with pyramidal symmetry. The structure can be expressed as Fe3 triangles in the ab plane, with P occupying the alternate layers. The unit cell of orthorhombic C23 structure has four formula units and shares a similar pseudo-hexagonal arrangement of iron atoms as in C22 structure, but the arrangement of P atoms is different from that of the hexagonal structure in that half of the P(II) atoms are neighboring empty Fe3 triangles along the c -direction [13].

Calculated ground state structural parameters and magnetic properties of Fe₂P for both C22 and C23 phases are listed in Table I, along with a comparison to earlier experimental data. For C22 structure, lattice parameters a and c are underestimated by $\sim 1\%$. For C23 the error in the estimation of a and c is $\sim 3\%$ and 2% respectively compared with the available experimental result [11], but the lattice constants are in good agreement with previous theoretical results [14]. Further, computed lattice constants under hydrostatic pressure of 30 GPa ($a = 5.39$, $b = 3.45$ and $c = 6.31$ Å) agree well with the reported experimental values [12] ($a = 5.38$, $b = 3.45$, $c = 6.42$ Å) under the same pressure.

Magnetic stabilization energy ($\Delta E^{\text{NM-FM}} = E^{\text{NM}} - E^{\text{FM}}$), evaluated as the difference between total energies of non-magnetic (NM) and ferromagnetic (FM) configurations, is 0.22 eV/f.u. for C22, which is in good agreement with the previous DFT result [21], and 0.18 eV/f.u. for C23 structure, for which there are no earlier reports for comparison. Thus our calculations establish the stability of FM configuration than NM for both phases of Fe₂P. Further, calculated total density of electronic states

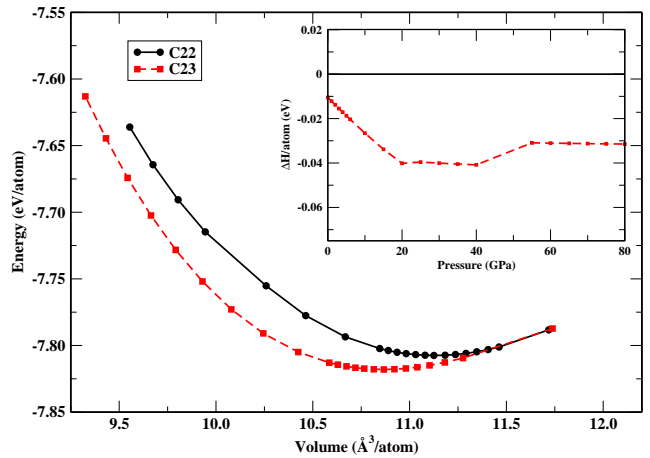


FIG. 1: (color online). Variation of energy as a function of volume for C22 and C23 phases of Fe₂P. The inset: calculated enthalpy of C23 phase with reference to C22 phase as a function of pressure.

(Fig. S1, Ref. [22]), corroborate the metallic and magnetic characteristics of both phases. Calculated magnetic moments for C22 phase are 0.82 and 2.23 μ_{B} for Fe(I) and Fe(II), respectively. The total magnetic moment per formula unit is 3.01 μ_{B} , owing to small moments induced at P sites due to the polarization effect of the Fe atoms, which are antiparallel to the Fe moments. These values are in good agreement with the previous experimental and theoretical results [20, 23–25]. For C23 phase, calculated magnetic moments are 0.18 and 1.61 μ_{B} for Fe(I) and Fe(II), respectively, and the total magnetic moment is 40% lower than that for C22 phase. Since experimental or theoretical data are not available for magnetic moments of C23 structure considered in the present work, we cannot make a comparison. However, the average magnetic moment per Fe atom (0.84 μ_{B}) is in reasonable agreement with the earlier DFT result (0.7 μ_{B}) [26].

Pressure dependent studies of materials are essential for the understanding of phase transition mechanism and structural stability. To examine the stability of Fe₂P under hydrostatic pressure, the total energy as a function of volume for both the phases of Fe₂P is determined and the results are shown in Fig. 1, together with enthalpy of C23 phase with reference to C22 phase as a function of hydrostatic pressure (inset of Fig. 1). Also, variation of magnetic moment with pressure is illustrated in Fig. S2 of Ref. [22]. As evident from the Fig. 1, no phase transformation occurs between C22 and C23 phase under compression up to 80 GPa. This is in disagreement with the computational results presented in the Ref. [26], where they predict C22 to C23 phase transformation under a pressure of 26 GPa. However, our results are in accordance with the experimental observations [12, 13], where C22 to C23 structural transformation under pressure is observed only when the samples are heated to higher temperatures of ~ 1400 K.

TABLE II: Calculated unit cell parameters for C22 and C23 phases of Fe₂P, using GGA, GGA+vdW, GGA+U, LDA and LDA+U along with experimental values for comparison.

	Expt. ^a	GGA	GGA+vdW	GGA+U	LDA	LDA+U
C22						
a (Å)	5.87	5.81	5.77	5.82	5.57	5.68
b (Å)	3.46	3.43	3.39	3.42	3.42	3.36
V (Å ³)	103.1	100.2	97.6	100.3	91.8	93.7
C23						
a (Å)	5.78	5.61	5.55	5.95	5.46	5.45
b (Å)	3.57	3.57	3.54	3.45	3.50	3.50
c (Å)	6.64	6.51	6.47	6.59	6.38	6.37
V (Å ³)	136.9	130.4	126.9	135.3	121.9	121.4
ΔE (meV/atom)	–	10.4	19.6	9.7	36.8	25.8

^a Experimental values are taken from Refs. [10] and [20] respectively for C22 and C23 phases.

As evident from the Fig. 1, C23 phase has lower energy than the C22 phase under the calculation conditions of absolute temperature and pressure, and the energy difference, i.e. $\Delta E_0 = E_0^{\text{C23}} - E_0^{\text{C22}}$ is calculated to be -10.4 meV/atom. To cross check this energy difference and to validate the functional used in our DFT calculations, we performed structural optimization using local density approximation (LDA). Also, calculations are carried out with on-site Hubbard corrections with $U = 2$ eV and $J = 0.95$ eV applied to Fe atoms [14] for both GGA (GGA+U) and LDA (LDA+U). Further, weak interlayer van der Waals interaction (GGA+vdW) is accounted using zero damping DFT-D3 method of Grimme [27]. The values are tabulated in Table II, which confirm our results obtained using GGA. Thus our DFT calculations predict C23 phase as the ground state structure of Fe₂P, under absolute conditions of temperature and pressure. This is in agreement with the theoretical results of Wu *et al.* [14], howbeit contradicting the experimental observation. A possible reason for the above discrepancy between experiments and theory could be zero-point vibrational energy contribution.

B. Phonons

To elucidate the role of zero-point vibrational energy with respect to the observed stability of C22 phase and to investigate local structural stability of the phases, full phonon dispersions for both phases are determined. Phonon dispersion and density of states for both phases are illustrated respectively in Figs. S3 and S4 of Ref. [22]. From figures, it is clear that both C22 and C23 phases are stable as these structures display no unstable modes. To examine the relative stability of Fe₂P phases at finite temperatures, we determine Helmholtz free energy. On the assumption that the entropy of the electronic part can be neglected, the Helmholtz free energy, F at volume V and temperature T can be approximated as [28]

$$F(V, T) = E_{\text{DFT}}(V) + F_{\text{vib}}(V, T), \quad (1)$$

where $E_{\text{DFT}}(V)$ is the total energy evaluated from the electronic structure calculations. $F_{\text{vib}}(V, T)$ is the vibrational contribution to the free energy given by the equation [29]

$$F_{\text{vib}}(V, T) = \frac{1}{2} \sum_{\text{qj}} \hbar \omega_{\text{qj}} + k_B T \sum_{\text{qj}} \ln [1 - \exp(-\hbar \omega_{\text{qj}} / k_B T)] \quad (2)$$

where T , k_B and \hbar respectively are temperature, Boltzmann constant and reduced Planck constant. ω_{qj} is phonon frequency of the phonon mode labelled by a set $\{\text{q}, \text{j}\}$, where q and j denotes wave vector and band index, respectively. The first term in the above equation is the zero-point vibration energy (EZPV), which is calculated to be 44.6 meV/atom and 49.2 meV/atom, respectively for C22 and C23 phases. Calculated F_{vib} and $F(V, T)$ as a function of temperature for both phases are shown in Fig. 2. It is clear from the figure that C22 phase becomes stable at ~ 300 K due to thermal vibrations and therefore confirms the stability of C22 phase over C23 phase under zero pressure conditions at room temperature. However, experimentally Fe₂P is reported to have C22 structure at temperatures down to 10 K [30]. This implies that the zero-point vibrational energy difference i.e. $\Delta E_{\text{ZPV}} = E_{\text{ZPV}}^{\text{C23}} - E_{\text{ZPV}}^{\text{C22}}$, which is calculated to be 4.6 meV/atom, favors C22 phase, yet not large enough to stabilize the C22 phase.

C. Spin fluctuations

From the above arguments, it is clear that electronic and vibrational energies together cannot explain the stability of C22 phase of Fe₂P, which is established as the stable phase by experiments at temperatures close to 0 K. Hence we have to seek for a distinct aspect of physics that has not been accounted so far in our calculations, but plays a key role in determining the ground state structure of Fe₂P. It is well known that in Fe-pnictide systems spin fluctuations are very important. For example, the pairing mechanism in recently discovered Fe-pnictide

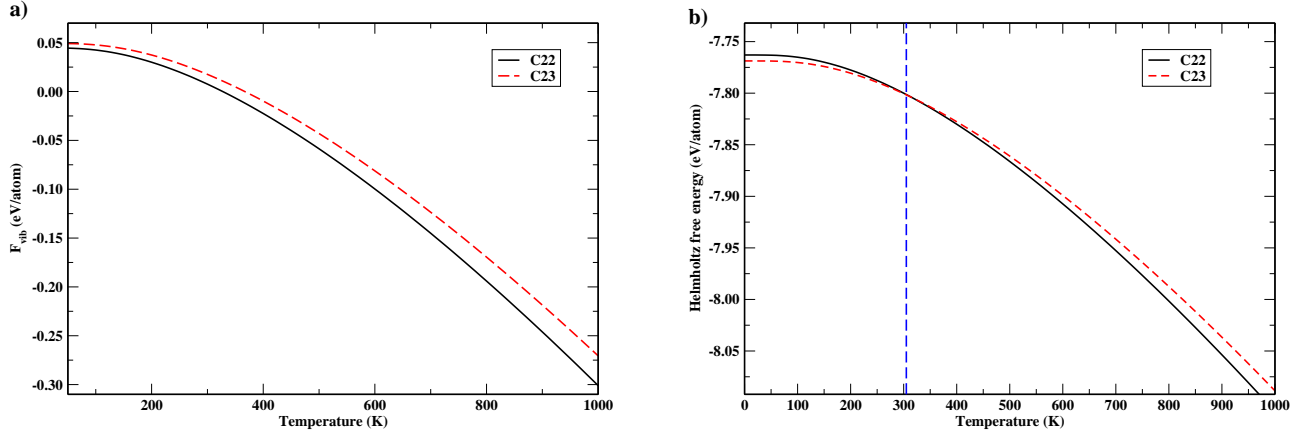


FIG. 2: (color online). Calculated (a) vibrational contribution to the free energy, and (b) Helmholtz free energy for C22 and C23 phases of Fe_2P .

based superconductors such as LaFePO , $\text{LaFeAsO}_{1-x}\text{F}_x$ etc. are explained through spin fluctuations [31–34]. Besides, for Si-doped Fe_2P , Delczeg-Czirjak *et al.* [35] reported zero-point spin fluctuation (ZPSF) energy difference to be large enough to stabilize the hexagonal phase over DFT predicted body centred orthorhombic phase. To explore whether C22 phase could possibly be stabilized by ZPSF at very low temperature, we write the total energy of the system as

$$E = E_{\text{DFT}} + E_{\text{ZPV}} + E_{\text{ZPSF}}, \quad (3)$$

where E_{DFT} is the electronic energy obtained from DFT calculation, E_{ZPV} is the energy correction due to zero-point vibration and E_{ZPSF} is zero-point spin fluctuation energy which is given by the equation [35–37] (refer APPENDIX A)

$$E_{\text{ZPSF}} = \frac{3\hbar}{4\pi} \omega_{\text{SF}} \ln(1 + (\omega_c/\omega_{\text{SF}})^2) \quad (4)$$

where ω_c is cutoff frequency and ω_{SF} is characteristic frequency of the spin fluctuation. In our study we use the approximations, $\hbar\omega_{\text{SF}} = \chi^{-1}\mu_{\text{B}}^2$ and $\hbar\omega_c \gg k_{\text{B}}T_{\text{melt}}$ [37], where χ and T_{melt} are magnetic susceptibility and melting temperature, respectively. In order to calculate E_{ZPSF} term, we determined total energy as a function of constrained magnetic moment for both phases of Fe_2P , as shown in Fig. 3.

The magnetic susceptibility χ is calculated using the relation [38]

$$\chi^{-1} = \left. \frac{\delta^2 E}{\delta M^2} \right|_{M=M_0}, \quad (5)$$

where E is the total energy evaluated from the electronic structure calculations, M is the magnetic moment and M_0 is its value at equilibrium. Considering the lower limit for cutoff frequency, $\hbar\omega_c = \hbar\omega_c^{\text{min}} = k_{\text{B}}T_{\text{melt}}$, we obtain ZPSF energy difference i.e. $\Delta E_{\text{ZPSF}} = E_{\text{ZPSF}}^{\text{C23}} -$

$E_{\text{ZPSF}}^{\text{C22}}$ equal to 23.6 meV/atom. Accordingly we can conclude that the ZPSF energy difference is large enough to overcome the DFT predicted energy difference (i.e. -10.4 meV/atom) and thus stabilizes the C22 phase. For the precise value of ZPSF energy, however, more accurate values of characteristic frequencies and cut-off frequencies are required. Typically, zero-point effects are crucial in the context of stability of layered or 2D materials such as boron nitride [39, 40]. However, our calculations disclose a rare case where quantum effects play pivotal role in the structural stability of a 3D material. Based on above arguments, we may predict the possibility of magnetic field induced structural quantum phase transition in Fe_2P . This work may provide a guide to further theoretical and experimental investigations on quantum phase transition in Fe_2P .

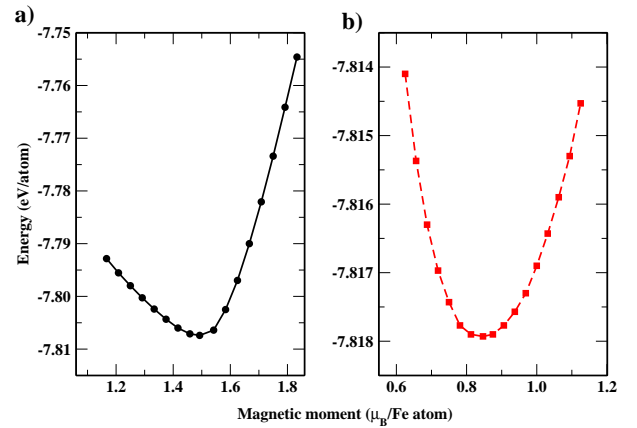


FIG. 3: (color online). Energy as a function of magnetic moment per Fe atom calculated for (a) C22, and (b) C23 phases of Fe_2P .

IV. CONCLUSIONS

In summary, we have systematically examined the ground state structural stability of Fe₂P with respect C22 and C23 phases, using first-principles calculations based on DFT. Calculated lattice parameters and magnetic properties for both phases agree well with experimental and theoretical results reported earlier. No phase transition between C22 and C23 phases is noticed under pure hydrostatic pressure, at 0 K temperature, in accordance with the experimental findings. Orthorhombic C23 phase is found to have lower energy than C22 phase, negating the experimental observation. Estimated zero-point vibrational energy is predicted to favor the C22 phase, yet insufficient to stabilize the hexagonal phase. The observed ground state stability of C22 phase is then attributed to lower ZPSF energy of C22 phase relative to C23. Thus, we present a unique result where quantum effects are found to significantly influence the structural stability of a bulk material. Experimental verification and deep theoretical understanding of the possible quantum phase transition can be envisioned as the future scope of this work.

ACKNOWLEDGEMENT

We acknowledge support from the Convergence Agenda Program (CAP) of the Korea Research Council of Fundamental Science and Technology (KRCF) and Global Knowledge Platform (GKP) program of the Ministry of Science, ICT and Future Planning.

APPENDIX A: DERIVATION OF THE ZERO POINT SPIN FLUCTUATION ENERGY TERM (E_{ZPSF})

Suppose \mathbf{m} is the total magnetic moment of the unit cell and let us consider that \mathbf{m} fluctuates around its mean value $\langle \mathbf{m} \rangle$. Therefore we can write,

$$\mathbf{m} = \langle \mathbf{m} \rangle + \delta \mathbf{m} \quad (\text{A.6})$$

The magnetic energy of the system can be expressed in terms of Ginzburg-Landau expansion,

$$\begin{aligned} E_{\mathbf{m}} &= a_0 + \frac{1}{2\chi} \mathbf{m}^2 + \frac{a_2}{4} \mathbf{m}^4 + \dots \\ &= a_0 + \frac{\langle \mathbf{m} \rangle^2}{2\chi} + \frac{a_2 \langle \mathbf{m} \rangle^4}{4} + \frac{\delta \mathbf{m}^2}{2\chi} + \dots \\ &\quad \frac{a_2 \delta \mathbf{m}^4}{4} + \frac{\delta \mathbf{m} \langle \mathbf{m} \rangle}{\chi} + \dots \end{aligned} \quad (\text{A.7})$$

where χ is the spin susceptibility of the system, which can be calculated using fixed moment calculations in the framework of the density functional theory [41] as shown in Sec. III C, and a_0 is the non-magnetic contribution to the energy. Now setting terms which are odd such as $\frac{\delta \mathbf{m} \langle \mathbf{m} \rangle}{\chi}$ to zero (as they would break the time reversal

symmetry) as well as neglecting the higher order terms, we get,

$$\begin{aligned} E_{\mathbf{m}} &= a_0 + \frac{\langle \mathbf{m} \rangle^2}{2\chi} + \frac{a_2 \langle \mathbf{m} \rangle^4}{4} + \frac{\delta \mathbf{m}^2}{2\chi} + \frac{a_2 \delta \mathbf{m}^4}{4} \\ &= E_{\langle \mathbf{m} \rangle} + E_{\text{SF}} \end{aligned} \quad (\text{A.8})$$

In the limit of small fluctuation ($\delta \mathbf{m} \rightarrow 0$) the spin fluctuation energy E_{SF} is given by,

$$E_{\text{SF}} \simeq \frac{1}{2\chi} \delta \mathbf{m}^2 \quad (\text{A.9})$$

The fluctuation can be split in to two parts,

$$\delta \mathbf{m}^2 = \delta \mathbf{m}_{\text{ZP}}^2 + \delta \mathbf{m}_{\text{Th}}^2 \quad (\text{A.10})$$

The first term in the Eq. A.10 is the zero temperature fluctuation, while the second term is due to fluctuation at finite temperature. Since we are interested only about the fluctuations close to 0 K, we can write,

$$E_{\text{ZPSF}} \simeq \frac{1}{2\chi} \delta \mathbf{m}_{\text{ZP}}^2 \quad (\text{A.11})$$

The remaining task is to calculate $\delta \mathbf{m}_{\text{ZP}}^2$, which can be related to dynamic spin susceptibility $\chi(q, \omega)$ via the fluctuation dissipation theorem given by,

$$\delta \mathbf{m}_{\text{ZP}}^2 = 3\hbar \int dq \int \frac{d\omega}{2\pi} \frac{1}{2} \text{Im} \chi(q, \omega) \quad (\text{A.12})$$

Now let us assume that all the fluctuations are localized near Fe-sites and therefore the spin susceptibility due to such fluctuations would be dispersion-less, i.e $\chi(q, \omega) \rightarrow \chi(\omega)$. The form of the dynamic spin susceptibility can be obtained from the Ref. [42] is given by,

$$\chi(\omega) = \frac{\chi}{1 - i\omega/\omega_{\text{SF}}} \quad (\text{A.13})$$

where χ is the frequency independent Kohn-Sham spin susceptibility, obtained from the fixed moment calculation. The Eq. A.12 now becomes,

$$\begin{aligned} \delta \mathbf{m}_{\text{ZP}}^2 &= \frac{3\hbar\chi}{4\pi} \int_0^{\omega_c} d\omega \frac{\omega/\omega_{\text{SF}}}{1 + (\omega/\omega_{\text{SF}})^2} \\ &= \frac{3\hbar\chi}{2\pi} \omega_{\text{SF}} \ln(1 + (\omega_c/\omega_{\text{SF}})^2) \end{aligned} \quad (\text{A.14})$$

where ω_{SF} is the characteristic frequency of the spin fluctuation and the energy integration is performed upto a cut-off frequency of ω_c . The spin-fluctuation energy is therefore given by from the Eq. A.11,

$$E_{\text{ZPSF}} = \frac{3\hbar}{4\pi} \omega_{\text{SF}} \ln(1 + (\omega_c/\omega_{\text{SF}})^2) \quad (\text{A.15})$$

The Eq. A.15 was used in the manuscript in order to estimate the contribution of spin fluctuation. We have not considered any anharmonic effects as we are interested in the temperature region far away from the magnetic transition temperature. It was pointed out in the previous study [42] that spin anharmonicity is important only near the magnetic transition temperature.

-
- [1] L. Caron, M. Hudl, V. Höglin, N. Dung, C. P. Gomez, M. Sahlberg, E. Brück, Y. Andersson, and P. Nordblad, *Physical Review B* **88**, 094440 (2013).
- [2] Y. Geng, Z. Zhang, O. Tegus, C. Dong, and Y. Wang, *Science China Materials* **59**, 1062 (2016).
- [3] M. Fries, L. Pfeuffer, E. Bruder, T. Gottschall, S. Ener, L. V. Diop, T. Gröb, K. P. Skokov, and O. Gutfleisch, *Acta Materialia*, 222 (2017).
- [4] Z. Gercsi, E. K. Delczeg-Czirjak, L. Vitos, A. Wills, A. Daoud-Aladine, and K. Sandeman, *Physical Review B* **88**, 024417 (2013).
- [5] M. Ai and K. Ohdan, *Journal of Molecular Catalysis A: Chemical* **159**, 19 (2000).
- [6] H. Zhao, D. Li, P. Bui, and S. Oyama, *Applied Catalysis A: General* **391**, 305 (2011).
- [7] S. N. Britvin, N. S. Rudashevsky, S. V. Krivovichev, P. C. Burns, and Y. S. Polekhovskiy, *American Mineralogist* **87**, 1245 (2002).
- [8] S. L. Brock and K. Senevirathne, *Journal of Solid State Chemistry* **181**, 1552 (2008).
- [9] M. Costa, O. Grånäs, A. Bergman, P. Venezuela, P. Nordblad, M. Klintenber, and O. Eriksson, *Physical Review B* **86**, 085125 (2012).
- [10] B. Carlsson, M. Gölin, and S. Rundqvist, *Journal of Solid State Chemistry* **8**, 57 (1973).
- [11] J. Senateur, A. Rouault, R. Fruchart, J. Capponi, and M. Perroux, *Materials Research Bulletin* **11**, 631 (1976).
- [12] P. Dera, B. Lavina, L. A. Borkowski, V. B. Prakapenka, S. R. Sutton, M. L. Rivers, R. T. Downs, N. Z. Boctor, and C. T. Prewitt, *Geophysical Research Letters* **35** (2008).
- [13] T. Gu, X. Wu, S. Qin, C. McCammon, and L. Dubrovinsky, *The European Physical Journal B* **86**, 311 (2013).
- [14] X. Wu and S. Qin, in *Journal of Physics: Conference Series*, Vol. 215 (IOP Publishing, 2010) p. 012110.
- [15] P. E. Blöchl, *Physical review B* **50**, 17953 (1994).
- [16] G. Kresse and J. Hafner, *Physical Review B* **47**, 558 (1993).
- [17] G. Kresse and J. Furthmüller, *Physical review B* **54**, 11169 (1996).
- [18] J. P. Perdew, K. Burke, and M. Ernzerhof, *Physical review letters* **77**, 3865 (1996).
- [19] A. Togo, F. Oba, and I. Tanaka, *Physical Review B* **78**, 134106 (2008).
- [20] D. Scheerlinck and E. Legrand, *Solid State Communications* **25**, 181 (1978).
- [21] H. P. Scott, B. Kiefer, C. D. Martin, N. Boateng, M. R. Frank, and Y. Meng, *High Pressure Research* **28**, 375 (2008).
- [22] See supplemental material at [URL will be inserted by the publisher] for supplementary figures and tables.
- [23] J. Tobola, M. Bacmann, D. Fruchart, S. Kaprzyk, A. Koumina, S. Niziol, J.-L. Soubeyroux, P. Wolfers, and R. Zach, *Journal of magnetism and magnetic materials* **157**, 708 (1996).
- [24] S. Ishida, S. Asano, and J. Ishida, *Journal of Physics F: Metal Physics* **17**, 475 (1987).
- [25] X. Liu, J. P. Liu, Q. Zhang, and Z. Altounian, *Physics Letters A* **377**, 731 (2013).
- [26] J. Nisar and R. Ahuja, *Physics of the Earth and Planetary Interiors* **182**, 175 (2010).
- [27] S. Grimme, J. Antony, S. Ehrlich, and H. Krieg, *The Journal of chemical physics* **132**, 154104 (2010).
- [28] Z. Lodziana and K. Parliński, *Physical Review B* **67**, 174106 (2003).
- [29] A. Togo and I. Tanaka, *Scripta Materialia* **108**, 1 (2015).
- [30] P. Jernberg, A. Yousif, L. Häggström, and Y. Andersson, *Journal of Solid State Chemistry* **53**, 313 (1984).
- [31] T. M. McQueen, M. Regulacio, A. J. Williams, Q. Huang, J. W. Lynn, Y. S. Hor, D. V. West, M. A. Green, and R. J. Cava, *Physical Review B* **78**, 024521 (2008).
- [32] D. J. Singh and M.-H. Du, *Physical Review Letters* **100**, 237003 (2008).
- [33] Y. Kohama, Y. Kamihara, M. Hirano, H. Kawaji, T. Atake, and H. Hosono, *Physical Review B* **78**, 020512 (2008).
- [34] Z.-J. Yao, J.-X. Li, and Z. Wang, *New Journal of Physics* **11**, 025009 (2009).
- [35] E. K. Delczeg-Czirjak, L. Delczeg, M. P. Punkkinen, B. Johansson, O. Eriksson, and L. Vitos, *Physical Review B* **82**, 085103 (2010).
- [36] A. Solontsov and D. Wagner, *Physical Review B* **51**, 12410 (1995).
- [37] A. Solontsov, V. Orlov, S. Kiselev, and A. Burmistrov, *Atomic energy* **107**, 263 (2009).
- [38] L. Ortenzi, I. I. Mazin, P. Blaha, and L. Boeri, *Physical Review B* **86**, 064437 (2012).
- [39] K. Albe, *Physical Review B* **55**, 6203 (1997).
- [40] J. Furthmüller, J. Hafner, and G. Kresse, *Physical review B* **50**, 15606 (1994).
- [41] W. F. Goh and W. E. Pickett, *Physical Review B* **96**, 079901 (2017).
- [42] A. Solontsov, *International Journal of Modern Physics B* **19**, 3631 (2005).